A NUMERICAL APPROACH FOR OPTIMIZATION OF CURING KINETICS OF COMPOSITE MATERIAL

A Thesis Submitted to
the Graduate School of Engineering and Sciences of
İzmir Institute of Technology
in Partial Fulfillment of the Requirements for the Degree of

MASTER OF SCIENCE

in Mathematics

by
Murat ÖZ

September 2021
İZMİR

ACKNOWLEDGMENTS

This thesis was made with the help and guidance of several people in making it available. I would like to express my special thanks to all of them.

First of all, I would like to express my gratidute to my supervisor, Prof. Dr. Gamze Tanoğlu, for his recommendation, patient, and encouragement during this thesis.

I would like to thank Dr. Fatih Türkmen for her advices and helps. Special thanks is extended to Dr. Neslişah İmamoğlu Karabaş for assist on editing my dissertation. Many thanks Dr. Yusufcan Uz to his help in obtaining various experimental results.

Additionally, I wish to thank İpek Palamut for unending spiritual support through all the hard times. Last, I warmly thank and appreciate my parents. They kept encouraging me when I encountered difficulty during the writing process of this thesis. Without their constant support, this accomplishment wouldn't have been made possible.

ABSTRACT

A NUMERICAL APPROACH FOR OPTIMIZATION OF CURING KINETICS OF COMPOSITE MATERIAL

In this thesis, we introduced a new method which is called the GMN (Gamze, Murat, Neslişah) algorithm. GMN algorithm determines the pre-exponential and activation energy of the curing process. This algorithm include tanh fitting for the measured conversion values via least squares minimization technique and linear fitting for the kinetic parameters. Experimentally determined differential scanning calorimetry (DSC) data sets for an epoxy resin functionalized by single wall carbon nanotubes are used for the verification of the proposed method. In computational part, in order to denote the effectiveness of the new proposed method, the results are also compared with the methods reported in the literature [21]. To sum up, we have shown that the GMN algorithm provides a good match with the experimental data for all kinetic parameters.

ÖZET

KOMPOZİT MALZEMEN İN KÜRELTME KİNETİĞİNİN OPTİMİZASYONU İÇİN SAYISAL BİR YAKLAŞIM

Bu tezde, kürleme işleminin ön üstel ve aktivasyon enerjisini belirlemek için yeni bir algoritma GMN (Gamze, Murat, Neslişah)sunduk. Bu metod ölçülen dönüşüm değerleri için tanh eğri uydurma yöntemi ile en küçük kareler minimizasyon yöntemlerinin kombinasyonun içerir ve kinetik parametre için liner eğri uydurma yöntemi kullanır. Sunulan yöntemin doğrulanması için tek duvarlı karbon nanotüpler tarafından işlenmemiş bir epoksi reçinesi için deneysel olarak belirlenmiş diferansiyel taramalı kalorimetri (DSC) veri setleri kullanılmıştır. Hesaplama kısmında, önerilen yeni yöntemin etkinliğini belirtmek için sonuçlar literatürde bildirilen yöntemlerle de karşılaştırılmıştır. Son olarak, GMN algoritması, kinetik parametrelerin hesaplanması için deneysel verilerle iyi bir tutarlılık içerinde olduğu elde edilmiştir.

TABLE OF CONTENTS

LIST OF FIGURES

Figure **Page**

Figure **Page**

Figure **Page**

LIST OF TABLES

CHAPTER 1

INTRODUCTION

1.1. Introduction

The aim of this thesis is the thermal characterization of laboratory-scale innovative carbon fiber/epoxy-based prepregs by incorporating single-wall carbon nanotubes (SWCNTs). Investigation of the cure behavior of a prepreg system is crucial for the characterization and optimization of the fiber reinforced polymeric (FRP) composite development. We will obtain a numerical solution for optimization of curing kinetics of composite material. We will mainly focus on curing kinetic modelling and optimization of reaction models.

We will deal with firstly the history of composite material and cure kinetic modelling. Over the past years, fiber reinforced polymeric (FRP) composites have been widely used for developing and manufacturing functional materials [4]. Prepreg based fiber reinforced composites include a combination of fiber and the polymeric matrix. For high performance and quality FRP composite manufacturing prepregs provide unique features such as being ready to use without any further processing, ease of use, high fiber volume fraction, uniform fiber alignment, accurate control of resin content, and very low void content [28, 17]. The demand for carbon fiber (CF) has shown an enormous increase and enabled the manufacturing of laminates with low density, low thermal expansivity, chemical inertness, high specific modulus, and specific strength [24]. CF-based prepregs have been produced using either hot melt process or solvent dip (solution impregnation) process which involves dissolving the resin in a solvent bath and dipping the reinforcing fabric in the resin solution.

Hybrid composites (also known as multiscale or hierarchical or nanostructured composites) consist of at least two reinforcements of different size scales. These rein-

forcements are generally applied as micro-scale continuous fibers and nano-scale fillers. An important feature of hybrid composites is that they take advantage of both the advantages of conventional fiber reinforced composites and the gain of feature and functionality by incorporating nanofillers into the matrix. Epoxy resins are the most preferred thermosetting polymers used as matrix bases in fiber reinforced composites due to their good thermal, electrical and mechanical properties [23]. One of the most notable considerations with the use of epoxy resin systems is their tendency to be brittle. [5]. The curing of epoxy matrices with these advantageous properties has been the subject of many studies such as high glass transition temperatures (Tg), high modulus and weight ratios [13, 14].

The mechanical and thermal properties of prepreg systems are linked to crosslinking reactions that occur during the epoxy curing process [27]. Epoxy resin is a thermosetting material that can form a three-dimensional network when it reacts with the hardener. Since it is an exothermic process, the heat of the reaction is released during the curing reaction. The curing mechanism is quite complicated as epoxy resin is subjected to many physical and chemical reactions during crosslinking [12, 8]. These chemical reactions play an important role in resin morphology, which determines the properties of cured thermoset resin and its composites. Since crosslinking continues after production, prepregs should be stored in a cold environment. In this way, it may be possible to extend the shelf life. The problem is the quality of end-product can be caused by using material that is over-cured or prepared with an unfavorable curing cycle. Therefore, one of the most important steps in the process of these incremental novel systems is the mechanism and kinetics involved in curing reactions. Cross-linking during the curing process can be monitored by Differential Scanning Calorimetry (DSC). The thermal analysis of partially cured prepreg samples by DSC provides generating a series of time-temperature-degree of cure diagrams. DSC can measure the heat during the exothermic or endothermic processes, providing information on cure and degradation reactions. Therefore, thermograms may be used to achieve high quality parts by optimizing kinetic parameters and curing cycles. There are two methods of thermal analysis kinetics, isothermal and non-isothermal methods. Non-isothermal methods have become the main method of thermal analysis kinetics due to their advantages.

In recent years, interest in the modeling of epoxy-based nanocomposite process-

ing has increased to obtain high quality parts by optimizing curing cycles and parameters [35, 3]. Thus, experimental studies for the cure cycles can be reduced to a minimum. Using nanofillers in the resin system may have a considerable impact on the heat of reaction, δH, degree of cure (α), and curing kinetics parameters, such as activation energy (E_α). Borchardt and Daniels [1] have obtained the kinetic parameters using a single DSC measurement. Moreover, Kissinger [16], Ozawa [22], Flynn–Wall–Ozawa [31] and Kissinger–Akahira–Sunose (KAS) [32] models have been used for multiple dynamic scans with more precision. Isoconversional (model-free) models are the types of kinetic models and provide information about kinetic analysis of solid-state reactions without an explicit kinetic model. It is very difficult to define the complete curing reaction of the epoxy resin system simply because many reactive processes take place at the same time. These models are useful for the study of complex curing processes. However, there are not many studies yet on how the material affects the curing mechanism as a result of the use of nanomaterials in hybrid prepreg systems. Siddiqui et al [29] studied the effect of multi-walled carbon nanotubes (MWCNTs) on the cure behavior of prepregs of carbon fiber-reinforced polymer (CFRP). The degree of the cure is lower for the prepregs containing 0.5–1.0 wt.% MWCNTs than neat prepregs. Costa et al [6] focused on understanding the cure behavior of the Carbon/epoxy 8552 thermoplastic toughened prepreg using DSC, DMA and rheometer. Dynamic DSC scans were performed to obtain kinetic parameters incorporating with nth order reaction model. The results showed that the heating rate more reliable to fabricate the polymeric composite is 2.5 $^\circ C$.min-1. Wu et. al. [37] analyzed that the high-temperature curing epoxy resin prepreg in fiber metal laminates using DSC. The kinetic event is related to the autocatalytic reaction patterns. The activation energy of the epoxy resin was 62.178kJ/mol and the reaction orders were 0.314 and 1.2157, the total reaction order was 1.5297. Kumar et al [18] studied cure cycle optimization of resin transfer molding type epoxy resin system containing MWCNTs for the manufacture of composite structures. Dynamic Mechanical Analysis (DMA) was performed to optimize the viscosity profile of the modified resin system.

The study of the curing behavior of a composite system is crucial for the mechanical characterization and optimization of fiber-reinforced polymeric (FRP) composite structure. Fiber reinforced composites, which have high strength properties from their

layered structure, pass many tests until the correct curing cycle is achieved. Therefore, one of the most important steps in the development of new composite systems is the mechanism and kinetics involved in curing reactions. In this thesis, an algorithm will be developed to approximate the parameters of the curing kinetics of the reaction model used according to certain parameters of the material. With successful modeling, experimental studies to calculate cure cycles will be minimized.

In this thesis will also be written using a hybrid Matlab algorithm using curve fitting and approximate solutions of differential equations of numerical analysis. The experimental results obtained by the mechanical engineering composite Laboratory in the doctoral study of doctoral student Yusuf Can Uz will be used to confirm this algorithm.

CHAPTER 2

MATHEMATICAL MODEL OF CURE KINETICS

This chapter introduces the basic concepts that will be used in the next chapters. Firstly, the idea of cure kinetic model is given. Then, we define Differential Scanning Calorimetry (DSC) to understanding of the cure process. Finally, numeric solution of model is defined in chapter 3.

2.1. Experimental

2.1.1. Materials

In this study, single-wall carbon nanotubes (SWCNTs) were supplied from Pinhas Inc., Turkey. SWCNTs were manufactured by TUBALL™, Luxembourg. The outer mean diameter of SWCNTs is below 2 nm, and their length is higher than 1μm. It contains high quality of SWCNT (G/D ratio > 90) with an iron content of less than 15%. The resin system used consisted of solvent-type epoxy F- RES21. The viscosity of the resin is 400-650 mPa.s at 25 $^{\circ}C$. 800 tex carbon fiber (A-49 filaments) were provided from DowAksa Inc., Turkey, and used as reinforcing constituent.

2.1.2. Sample Preparation

The forming defects on sidewalls of SWCNTs was performed by an oxidative process with strong acids (HNO3, H2SO4 1v:3v). As a result of the oxidation process, bonds with carboxylic acid (–COOH) were observed on the sidewalls of SWCNTs by FTIR spectroscopy. Single wall carbon nanotubes (SWCNTs) were called as F-SWCNTs after the covalent functionalization process. Multi-step dispersion technique was applied

for dispersing F-SWCNTs within the epoxy resin system. Firstly, F-SWCNTs were sonicated in the solvent (F-Prepreg) of the resin system for 15 minutes. Then, the solution was poured into epoxy resin (RES-21) and mixed by ultrasonication technique for 90 minutes. After the addition of the hardener, all the components of the resin system were mixed mechanically at 2000 rpm for 15 minutes. The resin system contained epoxy (RES 21), hardener (21 wt.% of epoxy), and its solvent (10 wt.% of whole resin system) and F-SWCNT. Finally, a modified resin system containing F-SWCNTs was ready for nano-engineered prepreg fabrication. Drum-type winding was applied by utilizing a solvent dip (solution impregnation) method using modified F-SWCNTs dispersed within the epoxy resin system and carbon filaments to produce laboratory-scale unidirectional (UD) prepregs with/without F-SWCNTs. The desired pattern per circuit was applied on the mandrel while impregnated in a bath with modified/unmodified resin. The hoop pattern, in which the winding angle is 90°, creates UD products. After the mandrel was completely wrapped to the desired thickness, the resin curing stage was reached. Approximately 750-850 grams of resin systems (resin, hardener, and its solvent) were used per production. After completion of the winding of the UD prepreg, the solvent was evaporated from the prepreg, and the resin reached B-stage using a drying oven according to the resin formulation. Prepregs had two different sides as dry and resin-rich side. Dimensions of the manufactured prepreg were 600 mm x 1000 mm.

2.1.3. Non-isothermal DSC

Differential scanning calorimetry (DSC) include thermal analysisy which measures the transformation of energy from a sample a physical or chemical change. [10] Temperature changes during curing determine the degree of cure of the system. The degree of hardening depends on the reaction temperature. The degree of curing process is changes the heat of reaction. The main idea of this technique is that when the sample undergoes a physical change as a result of chemical reaction, keeping the temperature of the sample may take more and less temperature values for the temperature as reference. These parameters are obtained using (DSC) and can be used to monitor the quality of

the final material. These parameters are obtained using differential scanning calorimetry (DSC) and can be used to monitor the quality of the final material. Samples we can define with the Shimadzu series which is consist of aluminum pans.

2.2. Kinetic Model

In the Differential scanning calorimetry measurements, the degree of cure α varies between 0 and 1 and is defined as follows [11]

$$\alpha = \frac{H_t}{\Delta H} \tag{2.1}$$

where H_t implies the amount of heat released in time t and ΔH implies the total heat of reaction. The area under the exothermic peak gives the amount of heat.
Usually, a kinetic model relates the rate of reaction $\frac{d\alpha}{dt}$ to some function of c and T. It is commonly accepted in the kinetic analysis of chemical reactions by thermal analysis that any chemical process of reaction will obey a rate law of the form

$$\frac{d\alpha}{dt} = k(T)f(\alpha) \tag{2.2}$$

where the functional dependence upon α is separated from the dependence upon T [30, 19]. Here $\frac{d\alpha}{dt}$ implies the rate of reaction, $k(T)$ is the dependent of temperature rate and is a constant, and $f(\alpha)$ defines our reaction model. The temperature dependence of the reaction rate is generally defined by an Arrhenius expression :

$$k(T) = Aexp(-\frac{E}{RT}) \tag{2.3}$$

in the equation, A is the pre-exponential factor and is a constant. E implies the activation energy, R refers to the universal gas constant and is a constant. T match up with to the absolute temperature.Thus, for a reaction sample using multiple linear regression,

it becomes possible to define the kinetic parameters obtained from isothermal and non-isothermal DSC exothermic measurements. When the process is isothermal, the temperature remains constant, but in non-isothermal conditions, the temperature usually rises relative to a constant heating rate

$$\beta = \frac{dT}{dt} \tag{2.4}$$

where β is the heating rate. Although the isothermal velocity expression obtained in isothermal measurements is more precise than the non-isothermal velocity expression, the DSC measurement is accurate. in general, less time consuming and thus more attractive than isothermal measurement. Combining the Eq. (2.2), (2.3) and (2.4) yields a resulting equation for non-isothermal conditions:

$$\frac{d\alpha}{dT} = \frac{A}{\beta} exp(-\frac{E}{RT}) f(\alpha) \tag{2.5}$$

Therefore, if the reaction model describing the data is known, we can predict the transformations obtained at a given temperature or heating rate by using the above equations. [21].

The activation energy of the curing reaction can be calculated by the isoconversional methods as Kissinger-Akahira-Sunose (KAS), and Kissinger which are the most cited algorithms in literature. Kissinger–Akahira–Sunose (KAS) Method [34]

$$\ln\left(\frac{\beta_i}{T_{\alpha,i}^2}\right) = Const - \frac{E_\alpha}{RT_\alpha} \tag{2.6}$$

Kissinger Method:

$$\ln\left(\frac{\beta_i}{T_p^2}\right) = Const - \frac{E}{RT_p} \tag{2.7}$$

	Code	Reaction model	$f(\alpha)$	$g(\alpha)$
1	P4	Power law	$4\alpha^{3/4}$	$\alpha^{1/4}$
2	P3	Power law	$3\alpha^{2/3}$	$\alpha^{1/3}$
3	P2	Power law	$2\alpha^{1/2}$	$\alpha^{1/2}$
4	P2/3	Power law	$2/3\alpha^{-1/2}$	$\alpha^{3/2}$
5	D1	One-dimensional diffusion	$1/2\alpha^{-1}$	α^{2}
6	F1	Mampel (first-order)	$1-\alpha$	$-\ln(1-\alpha)$
7	A4	Avrami-Erofeev	$4(1-\alpha)[-\ln(1-\alpha)]^{3/4}$	$[-\ln(1-\alpha)]^{1/4}$
8	A3	Avrami-Erofeev	$3(1-\alpha)[-\ln(1-\alpha)]^{2/3}$	$[-\ln(1-\alpha)]^{1/3}$
9	A2	Avrami-Erofeev	$2(1-\alpha)[-\ln(1-\alpha)]^{1/2}$	$[-\ln(1-\alpha)]^{1/2}$
10	D3	Three-dimensional diffusion	$2(1-\alpha)^{2/3}[1-(1-\alpha)^{1/3}]^{-1}$	$[1-(1-\alpha)^{1/3}]^{2}$
11	R3	Contracting sphere	$3(1-\alpha)^{2/3}$	$1-(1-\alpha)^{1/3}$
12	R2	Contracting cylinder	$2(1-\alpha)^{1/2}$	$1-(1-\alpha)^{1/2}$
13	D2	Second-order	$(1-\alpha)^{2}$	$(1-\alpha)^{-1}-1$

Figure 2.1. Chosen kinetic models to describe activated processes.

Different approaches can be found in the literature to explain the reaction processes of thermoset materials. Most can be divided into model-fit and model-less approaches. The latter are also called isoconversional methods. Using the model fitting approach to explain the reaction kinetics, a reaction model $f(\alpha)$ which is a conversion-dependent function is used. $g(\alpha)$ is a integral form of $f(\alpha)$. Some of these kinetic models are listed in Table 2.1. These methods are widely used in different fields. Predicting the degree of cure as the reaction progresses is very important for isothermal cure measurements.The first formula can be modified to calculate the degree of cure as follows:

$$\alpha = \frac{\Delta H_T - \Delta H_R}{\Delta H_R} \tag{2.8}$$

where ΔH_T equals the total enthalpy of reaction measured at a certain heating rate for an unreacted sample, and ΔH_R is the residual heat of the reaction for the isothermally cured sample for a certain period of time. This formula will allow us to calculate the degree of improvement as treatment progresses. It is also important to develop a relationship between α and T, as T provides a better value for observing treatment progress.

Table 2.1. Experimental data from Sample 1

Time sec	$Temp$ C	ΔH mJ/g	$Time_{Ht}$	Ht mJ/g	Weight mg	Conversion	Heat flow W/g	Time const sec	Time α
0	18.27	−0.08	133.1	358.3126	3.9	0	−0.027586207	270	0
6	19.58	−0.12	45.89	358.3126		0.000220135	−0.041379312		6
12	21.52	−0.48		358.3126		0.000913223	−0.165517241		12
18	23.55	−0.81		358.3126		0.002115477	−0.279310345		18
24	25.59	−0.98		358.3126		0.003770774	−0.337931034		24
30	27.63	−1.06		358.3126		0.005806386	−0.365517241		30
36	29.67	−1.11		358.3126		0.00828024	−0.382758621		36
42	31.7	−1.14		358.3126		0.011428775	−0.393103448		42
48	33.74	−1.17		358.3126		0.015530503	−0.403448276		48
54	35.77	−1.2		358.3126		0.020751615	−0.413793103		54
60	37.8	−1.23		358.3126		0.027249061	−0.424137931		60
66	39.83	−1.26		358.3126		0.035381217	−0.434482759		66
72	41.86	−1.29		358.3126		0.045713449	−0.444827586		72
78	43.89	−1.33		358.3126		0.058734636	−0.458620693		78
84	45.92	−1.37		358.3126		0.074752367	−0.472413793		84
90	47.95	−1.39		358.3126		0.09415447	−0.479310345		90
96	49.98	−1.39		358.3126		0.117545905	−0.479310345		96
102	52	−1.38		358.3126		0.145587453	−0.475862069		102
108	54.03	−1.37		358.3126		0.178775056	−0.472413793		108
114	56.06	−1.37		358.3126		0.21734861	−0.472413793		114
120	58.08	−1.36		358.3126		0.261201953	−0.468965517		120
126	60.11	−1.36		358.3126		0.309782194	−0.468965517		126

CHAPTER 3

NUMERICAL SOLUTION OF MODELS

In this chapter, we take a look how to solution of Cure Kinetic Model and we will concentre their solution method. Cure kinetic model has no analytical solution, therefore we have to define approximations and numerical methods to solve model [33]. First of all, we explain numerical differential equation which is used to find numerical approximations to the solutions of differential equations. Then we define curve fitting method is theoretically describe experimental data to find the parameters associated with this model.

3.1. Numerical Differential Equation

In this section, we will give the brief description about what a numeric differential equation look like.

An ordinary differential equation is an equation that specifies the derivative of a function $y : \mathbb{R} \longrightarrow \mathbb{R}$ as

$$y'(x) = f(x, y(x)), \tag{3.1}$$

where

$$y' = \frac{dy}{dx} \tag{3.2}$$

we generally use x to denote the 'independent' or 'time' variable and y to denote the 'dependent variable'. More generally, an nth order ordinary differential equation

specifies the nth derivative of a function as

$$y_n(x) = f(x, y(x), \ldots, y^{n-1}(x)) \tag{3.3}$$

We will analyze for a solution to (3.2) for $x > x_0$ as

$$y(x_0) = b \tag{3.4}$$

where $x_0 < x < b$, x_0 and b are two real numbers. The fist order differential equation (3.2) with the initial condition described in (3.4) is called the Initial Value Problem. Analytical solution is defined by $y(x)$, and approximate solution is represented by y_n [2].

3.1.1. Runge-Kutta Method

The Runge-Kutta method is known to be a common method to solve the initial value problem, and it provides very important accuracy compared to other methods, so it is of great importance. Additionally requires only a single assessment of $f(x_n, y_n)$ to get y_{n+1} from y_n. The Runge-Kutta method has a considerably higher accuracy than other methods and has faster convergence rates.

3.1.1.1. Definition of Runge-Kutta Method

Consider the first-order ODE of the form given by

$$\frac{dy}{dx} = f(x, y), \tag{3.5}$$

with initial condition $y(x_0) = y_0$ The general form of the Runge-Kutta method is

$$y_{n+1} = y_n + h\Phi(x_n, y_n; h), \qquad n = 0, 1, \ldots, N-1 \tag{3.6}$$

where $\Phi(x_n, y_n; h)$ is an increment function on the our interval $[x_n, x_{n+1}]$ and $h = \frac{x_{n+1}-x_n}{N}$ is the step size. We can define its general form like

$$\Phi(x, y; h) = \sum_{r=1}^{R} b_r k_r, \tag{3.7}$$

b_r's are the constant weight coefficients and k_n's are the coefficients to be calculated.

$$\begin{aligned}
k_1 &= f(x_n, y_n) \\
k_2 &= f(x_n + c_2 h, y_n + a_{21} k_1 h) \\
&\vdots \\
k_r &= f(x_n + h c_r, y_n + h \sum_{s=1}^{r-1} b_{rs} k_s), \qquad r = 2, \ldots, R \\
c_r &= \sum_{s=1}^{r-1} a_{rs}, \qquad r = 2, \ldots, R
\end{aligned}$$

In this, for each of the function k's are symbolize slope of the solution which are approximated to $y(x)$. The coefficients a_r, c_r, k_r define the numerical method. These are normally arranged in Butcher tableau:

$$\begin{array}{c|c} c & A \\ \hline & b^T \end{array}$$

The coefficient b^T is a vector of quadrature weights, and $a_{ij} = (1, \ldots, s)$ defines the matrix A [9].

3.1.1.2. Explicit Runge Kutta-Method

We can define the R-stage Explicit Runge-Kutta method like

$$y_{n+1} = y_n + \sum_{i=1}^{R} b_i k_i \tag{3.8}$$

where

$$\begin{aligned} k_1 &= f(x_n, y_y) \\ k_i &= f(x_n + c_i h, y_n + \sum_{j=1}^{R-1} a_{ij} k_i), \qquad i = 1, 2, \ldots R \end{aligned}$$

where $h = \frac{x_{n+1} - x_n}{N}$.
If Runge-Kutta method is consistent, the following condition must be satisfied

$$\sum_{j=1}^{i-1} a_{ij} = c_i, \qquad i = 2, \ldots, R \tag{3.9}$$

Simple representation of Runge-Kutta method is known as the (Explicit) Euler method. We can describe One-stage Runge-Kutta methods ($R = 1$).

$$y_{n+1} = y_n + hf(x_n, y_n)$$

we can formed as shown their tableau

0	0
	1

Moreover, Runge-Kutta method is known as midpoint method which is called a second-order method ($R = 2$).

$$y_{n+1} = y_n + hf(x_n + \frac{1}{2}h, y_n + \frac{1}{2}hf(x_n, y_n))$$

and their tableau

0	0	
$\frac{1}{2}$	$\frac{1}{2}$	0
	0	1

For calculating $y(x_{n+1})$, higher order of derivatives is necessary to expand at the Taylor series.

$$y(x_{n+1}) = y(x_n) + hy'(x_n) + \frac{1}{2!}h^2y''(x_n) + \cdots + \frac{1}{p!}h^py^{(p)}(x_n) \tag{3.10}$$

Differentiating the differential equation $y'(x) = f(x, y(x))$ with respect to using the chain rule gives

$$y''(x) = f_x + y'f_y = f_x + ff_y \tag{3.11}$$

We get

$$y(x_{n+1}) = y(x_n) + hf + \frac{1}{2}h^2f_yf + O(h^3) \tag{3.12}$$

The second-order approximate solution of the Runge-Kutta method can be obtained

$$y_{n+1} = y_n + [b_1k_1 + b_2k_2] \tag{3.13}$$

where

$$k_1 = f(x_n, y_n) = f \tag{3.14}$$

$$k_2 = f(x_n + c_2h, y_n + ha_{21}k_1) = f + ha_{21}ff_y \tag{3.15}$$

then, if we put that in Eqn.(3.13)

$$y_{n+1} = y_n + [b_1 f + b_2(f + ha_{21} f f_y)] \tag{3.16}$$

Now, if we match Eqn.(3.40) with Taylor series Eqn.(3.10), we will obtain the following equations

$$\begin{aligned} b_1 + b_2 &= 1 \\ b_2 a_{21} &= \frac{1}{2} \end{aligned}$$

In this case we take $b_1 = 0, b_2 = 1$ and $a_{21} = \frac{1}{2}$, we will obtain the modified Euler method:

$$y_{n+1} = y_n + hf(x_n + \frac{1}{2}h, \frac{1}{2}hf(x_n, y_n) \tag{3.17}$$

Furthermore if we choose $b_1 = 0, b_2 = 1$ and $a_{21} = 1$, we will obtain the improved Euler method:

$$y_{n+1} = y_n + \frac{1}{2}h[f(x_n, y_n) + f(x_n + h, y_n + hf(x_n, y_n)] \tag{3.18}$$

3.1.1.3. Implicit Runge-Kutta Method

The form of R stage Runge-Kutta method is known like

$$y_{n+1} = y_n + h \sum_{i=1}^{R} b_i k_i \tag{3.19}$$

where

$$k_i = f(x_n + c_i h, y_n + h \sum_{j=1}^{R} a_{ij} k_j), \qquad i = 1, \ldots, R \tag{3.20}$$

and we can define their Butcher tableau as follows

$$\begin{array}{c|cccc} c_1 & a_{11} & a_{12} & \dots & a_{1r} \\ c_2 & a_{21} & a_{22} & \dots & a_{2r} \\ \vdots & \vdots & \vdots & \ddots & \vdots \\ c_r & a_{r1} & a_{r2} & \dots & a_{rr} \\ \hline & b_1 & b_2 & \dots & b_r \end{array}$$

Implicit Runge-Kutta method is obviously much more complicated than explicit version. The complexity can be justified by improved stability and higher order.

3.1.1.4. Fourth Order Runge-Kutta Method

We can explain the Fourth Order Runge-Kutta method, which is the most important method, as follows

$$y_{n+1} = y_n + \frac{1}{6}(k_1 + 2k_2 + 2k_3 + k_4) \tag{3.21}$$

where

$$\begin{aligned} k_1 &= f(x_n, y_n) \\ k_2 &= f(x_n + \frac{1}{2}h, y_n + \frac{1}{2}hk_1h) \\ k_3 &= f(x_n + \frac{1}{2}h, y_n + \frac{1}{2}hk_2h) \\ k_4 &= f(x_n + \frac{1}{2}h, y_n + k_3h) \end{aligned}$$

The Fourth Degree Runge-Kutta method is crucial important and most well-known of all Runge Kutta methods. Their tableau as follows

$$\begin{array}{c|cccc} 0 & & & & \\ \frac{1}{2} & \frac{1}{2} & & & \\ \frac{1}{2} & 0 & \frac{1}{2} & & \\ 1 & 0 & 0 & 1 & \\ \hline & \frac{1}{6} & \frac{1}{3} & \frac{1}{3} & \frac{1}{6} \end{array}$$

The local truncation error is $O(h^5)$ and this is the most important. Also, it has four evaluation of function for each step [15].

3.1.1.5. Convergence and Stability Condition of Fourth-order Runge-Kutta Method

Söderlind [1] emphasizes that the stability property has a crucial role in solving first-order ODEs using numerical methods.

$$\frac{d\alpha}{dT} = f(T, \alpha), \qquad \alpha(T_0) = \alpha_0 \tag{3.22}$$

If we consider the integral form of 3.22 equation

$$\alpha_n = \alpha_{n+1} + \int_{T_n}^{T_{n+1}} f(T, \alpha) dT \tag{3.23}$$

We obtain Runge-Kutta formula has order 4, so it will be possible to approximate the integral $\int_{T_n}^{T_{n+1}} f(T, \alpha) dT$ by using a numerical method with truncation error of $O(h^5)$. The Simpson's rule is fits for this condition.

Simpson's rule in the form of quadratic interpolation is used to obtain the Runge-Kutta formula in a form similar to the initial value problem [36]. The equation is shown below:

$$\int_{T_n}^{T_{n+1}} f(T)dT = \frac{h}{6}\left[(T_n + 2f\left(\frac{T_n + T_{T+1}}{2}\right) + f(T_{n+1})\right] + \epsilon \tag{3.24}$$

where the cut error is $\epsilon = -\frac{1}{90}f^4(\psi, \alpha)h^5$, and $\epsilon \in (T_n, T_{n+1})$
Consequently, the form of Fourth-order Runge-Kutta formula can be illustrated as below

$$\begin{aligned}
K_1 =& f(T_{n-1}, \alpha_{n-1}) \\
K_2 =& f(T_{n-1} + \frac{1}{2}h, \alpha_{n-1} + \frac{h}{2}K_1) \\
K_3 =& f(T_{n-1} + \frac{1}{2}h, \alpha_{n-1}\frac{h}{2}K_2) \\
K_4 =& f(T_{n-1} + h, \alpha_{n-1} + h(aK_1 + bK_2 + cK_3)) \\
\alpha_n =& \alpha_{n-1} + \frac{h}{6}(K_1 + 2K_2 + 2K_3 + K_4)
\end{aligned} \tag{3.25}$$

To determine the unknown coefficients, the stability analysis is used:

$$\begin{aligned}
K_1 =& (-\lambda)\alpha_{n-1} \\
K_2 =& (-\lambda + \frac{1}{2}\lambda^2 h)\alpha_{n-1} \\
K_3 =& (-\lambda + \frac{1}{2}\lambda^2 h - \frac{1}{4}\lambda^3 h^2)\alpha_{n-1} \\
K_4 =& (-\lambda + \lambda^2 h + \frac{1}{2})\lambda^3 h^2 - \frac{1}{4}\lambda^4 h^3)\alpha_{n-1}
\end{aligned}$$

Then we can obtain the following equation:

$$\alpha_{n+1} = \alpha_n + \frac{1}{6}\left[1 - \lambda h + \frac{1}{2}\lambda^2 h^2 - \frac{1}{6}\lambda^3 h^3 + \frac{1}{24}\lambda^4 h^4\right]\alpha_{n-1} \tag{3.26}$$

Comparing with the corresponding Taylor's formula:

$$\alpha_n = \alpha_{n+1} + \left[\lambda h + \frac{1}{2!}\lambda^2 h^2 + \frac{1}{3!}\lambda^3 h^3 + \frac{1}{4!}\lambda^4 h^4\right]\alpha_{n+1} \tag{3.27}$$

The increment function of Eqn.(3.25)

$$\Phi(T, \alpha, h) = \frac{1}{6}\left[k_1(T, \alpha, h) + 2k_2(T, \alpha, h) + 2k_3(t, \alpha, h) + k_4(T, \alpha, h)\right] \tag{3.28}$$

where

$$\begin{aligned} k_1(T, \alpha, h) =& f(T, \alpha) \\ k_2(T, \alpha, h) =& f(T + \frac{1}{2}h, \alpha + \frac{h}{2}k_1(T, \alpha, h)) \\ k_3(T, \alpha, h) =& f(T + \frac{1}{2}h, \alpha\frac{h}{2}k_2(t, \alpha, h)) \\ k_4(T, \alpha, h) =& f(T + h, \alpha + hk_3(T, \alpha, h)) \end{aligned} \tag{3.29}$$

According to Lipschitz Condition:

$$|k_1(T, \alpha_1, h) - k_2(T, \alpha_2, h)| \leq L|\alpha_1 - \alpha_2| \tag{3.30}$$

$$\begin{aligned} |k_2(T, \alpha_1, h) - k_2(T, \alpha_2, h)| \leq& L\left(|\alpha_1 - \alpha_2| + \frac{1}{2}hL|\alpha_1 - \alpha_2|\right) \\ =& L(1 + \frac{1}{2}h)|\alpha_1 - \alpha_2| \end{aligned} \tag{3.31}$$

$$|k_3(T,\alpha_1,h) - k_3(T,\alpha_2,h)| \leq L(|\alpha_1 - \alpha_2| + \frac{1}{2}hL(1+\frac{1}{2}h)|\alpha_1 - \alpha_2|) \tag{3.32}$$

$$= L(1 + \frac{1}{2}hL + (\frac{1}{2}h)^2)|\alpha_1 - \alpha_2|$$

$$|k_4(T,\alpha_1,h) - k_4(T,\alpha_2,h)| \leq L\left(|\alpha_1 - \alpha_2| + hL(1 + \frac{1}{2}hL + (\frac{1}{2}h)^2)|\alpha_1 - \alpha_2|\right) \tag{3.33}$$

$$= L(1 + hL + \frac{1}{2}(hL)^2 + \frac{1}{4}(hL)^3)|\alpha_1 - \alpha_2| \tag{3.34}$$

we can get the inequality:

$$|\Phi(T,\alpha_1,h) - \Phi(T,\alpha_2,h)| \leq L\left[1 + \frac{1}{2}hL + \frac{1}{6}h^2L^2 + \frac{1}{24}h^3L^3\right]|\alpha_1 - \alpha_2| \tag{3.35}$$

We have assume that

$$\tilde{L} = L\left[1 + \frac{1}{2}hL + \frac{1}{6}h^2L^2 + \frac{1}{24}h^3L^3\right] \tag{3.36}$$

where L implies Lipschitz constant, h represent the step size and the problem is called to be convergent if $\tilde{L} > 0$. Clearly, the condition could be satisfied by an appropriate hL.
The solution of the inequality $\tilde{L} > 0$ is [25]

$$hL > -2.7853 \tag{3.37}$$

The inequality Eqn.(3.37) always holds.
The stability condition of Runge-Kutta Method the same way is obtained in Eqn.(3.27).

$$\left[1 - \lambda h + \frac{1}{2}\lambda^2 h^2 - \frac{1}{6}\lambda^3 h^3 + \frac{1}{24}\lambda^4 h^4\right] < 1 \tag{3.38}$$

The stability function of Runge-Kutta Method is

$$S(\lambda h) = 1 - \lambda h + \frac{1}{2}(\lambda h)^2 - \frac{1}{6}(\lambda h)^3 + \frac{1}{24}(\lambda h)^4 \tag{3.39}$$

3.1.1.6. Existence and Uniqueness Theorem

Theorem 3.1 *(Gronwall's Inequality)*

Let α, β and c be non-negative constants, and $u, f : [\alpha, \beta] \longrightarrow [0, \infty]$ continuous. If,

$$u(t) \leq c + \int_{\alpha}^{t} f(s)u(s)ds, \qquad \alpha \leq \beta,$$

then

$$u(t) \leq ce^{\int_{\alpha}^{t} f(s)ds}, \qquad \alpha \leq \beta.$$

Theorem 3.2 *(ODE Uniqueness)*

Let $f(x, y) = (f_1(x, y), f_2(x, y), ..., f_n(x, y))^{tr}$ be a vector function whose components are each continuous in both x and y in some neighborhood $a \leq x \leq b$ and $a_1 \leq y_1 \leq b_1, a_2 \leq y_2 \leq b_2, \ldots, a_n \leq y_1 \leq b_n$ and whose partial derivative $\partial_{yl} f_k(x, y)$ are continuous in both x and y in the same neighborhoods for each l, $k = 1, ..., n$. Then given any initial point $(x_0, y_0) \in R \times R^n$ such that $a < x_0 < b$ and $a_k < y_{0k} < b_k$ for all $k = 1, ..., n$ any solution to IVP

$$\begin{aligned} y'(x) &= f(x, y) \\ y(x_0) &= y_0 \end{aligned} \tag{3.40}$$

is unique on the neighborhood of continuity [9].

Consider the our kinetic model

$$\frac{d\alpha}{dT} = \frac{A}{\beta} exp(-\frac{E}{RT}) f(\alpha), \qquad \alpha(T_0) = \alpha_0 \tag{3.41}$$

In the literature there are different choice of $f(\alpha)$. For the model most suitable choice is

$$f(\alpha) = \alpha^m (1-\alpha)^n, \qquad m+n = 2$$

and suppose that we want to estimate uniqueness on the intervals for sample1 and $\alpha \in (0,1)$.

$$\frac{d\alpha}{dT} = F(\alpha(T)) \tag{3.42}$$

We begin by supposing that $\alpha_1(T)$ and $\alpha_2(T)$ represent two solutions of the Eqn.(3.41).

$$\alpha_1(T) = F(\alpha_1(T))$$
$$\alpha_2(T) = F(\alpha_2(T))$$

$$\begin{aligned} |\alpha_1(T) - \alpha_2(T)| &\leq \int_{T_0}^{T} |F(\alpha_1(s)) - F(\alpha_2(s))| ds \\ &\leq \int_{T_0}^{T} L \frac{dF}{d\alpha} |\alpha_1(s) - \alpha_2(s)| ds \end{aligned}$$

we can calculate $\frac{dF}{d\alpha}$

$$\begin{aligned} \frac{dF}{d\alpha} =& \frac{A}{\beta} exp(-\frac{E}{RT}) f(\alpha) \\ =& f(\alpha) = \alpha^{0.6}(1-\alpha^{1.4}) \\ \frac{df}{d\alpha} =& -\frac{((1-\alpha)^{(2/5)}(10\alpha - 3))}{5\alpha^{(2/5)}} \end{aligned}$$

and $0 < \alpha < 1$.

L is the Lipchitz condition and we can reorganize that

$$V(T) = |\alpha_1(T) - \alpha_2(T)|$$

and

$$V(T) \leq \int_{T_0}^{T} LV(s)ds$$

from Gronwall's Inequality we can poof that

$$V(T) \leq 0 + \int_{T_0}^{T} LV(s)ds$$

and

$$\begin{aligned} |V(T)| \leq & ce^{L\int_{T_0}^{T} V(s)ds} \\ \leq & 0e^{L\int_{T_0}^{T} V(s)ds} = 0 \end{aligned}$$

and we from definition of $V(T)$ we know that

$$V(T) = |\alpha_1(T) - \alpha_2(T)| = 0 \qquad \alpha_1(T) = \alpha_1(T)$$

Theorem 3.3 *(Banach fixed point theorem)*

Let V be a Banach space, let $K \subset V$ be a closed subset, and let $F : X \longrightarrow X$ be a contraction ($0 < q < 1$) such that

$$\|F(x) - F(y)\| \leq q\|x - y\| \qquad for \quad all \quad x, y \in X.$$

holds. Then the following conclusions hold:

1.) *F has a unique fixed point $x_* \in K$ i.e $F(x_*) = x_*$.*

2.)*For any $x_0 \in X$ the sequence $x_{n+1} = F(x_n)$ converges to x_**

Consider the our kinetic model Eqn.(3.46) and suppose we want to establish existence on the intervals for sample 1 and $0 \leq \alpha \leq 1$, with $T_0 \in T$ and $\alpha \in (0, 1)$.

$$\frac{d\alpha}{dT} = V(\alpha(T))$$

$$\begin{aligned}\alpha(T) =& \alpha_0 + \int_{T_0}^{T} V(\alpha(T)) \\ \alpha(T) =& F(\alpha(T))\end{aligned}$$

Since F is a contraction mapping, we have that for all $\epsilon > 0$ there exists an $M \in N$ such that

$$||\alpha_{k+m} - \alpha_k|| < \epsilon \qquad for \quad all \quad k > M \quad and \quad all \quad m > 0.$$

To indicate this, choose some k and $m \in N$ and investigate that

$$\begin{aligned}||\alpha_{k+m} - \alpha_k|| =& ||\alpha_{k+m} + \sum_{j=1}^{m-1}(\alpha_{k+j} - \alpha_{k+j}) - \alpha_k|| \\ &\leq \sum_{j=1}^{m} ||(\alpha_{k+j} - \alpha_{k+j-1})||\end{aligned}$$

From $\alpha_{k+j} = F(\alpha_{k+j-1})$ one has

$$||\alpha_{k+j} - \alpha_{k+j-1}|| = ||F(\alpha_{k+j-1}) - F(\alpha_{k+j-2})|| \leq q||\alpha_{k+j-1} - \alpha_{k+j-2}||$$

also,

$$||\alpha_{k+j-1} - \alpha_{k+j-2}|| = ||F(\alpha_{k+j-2}) - F(\alpha_{k+j-3})|| \leq q||\alpha_{k+j-3} - \alpha_{k+j-4}||$$

such that

$$\|\alpha_{k+j} - \alpha_{k+j-1}\| = \|F(\alpha_{k+j-1}) - F(\alpha_{k+j-2})\| \leq q^2\|\alpha_{k+j-3} - \alpha_{k+j-4}\|$$

Thus, such a conclusion can be reached by induction:

$$\|\alpha_{k+j} - \alpha_{k+j-1}\| = \|F(\alpha_{k+j-1}) - F(\alpha_{k+j-2})\| \leq \cdots \leq q^{j-1}\|\alpha_{k+1} - \alpha_k\|$$

Substituting back to the inequality we obtain

$$\|\alpha_{k+m} - \alpha_k\| = \sum_{j=1}^{m} \|\alpha_{k+j} - \alpha_{k+j-1}\| \leq \sum_{j=1}^{m} q^{j-1}\|\alpha_{k+1} - \alpha_k\| \tag{3.43}$$

Sum of geometric series is used here:

$$\sum_{j=1}^{\infty} p^{j-1} = \frac{1}{1-q}$$

Also, we know that

$$\|\alpha_{k+1} - \alpha_k\| = \|F(\alpha_{k+1}) - F(\alpha_k)\| \leq q\|\alpha_k - \alpha_{k-1}\| \leq q^2\|\alpha_{k-1} - \alpha_{k-2}\|$$

which leads us to

$$\|\alpha_{k+j} - \alpha_{k+j-1}\| \leq q^k\|\alpha_1 - \alpha_0\|$$

With Eqn.(3.43) this gives:

$$\|\alpha_{k+m} - \alpha_k\| \leq \frac{q^k}{1-q}\|\alpha_1 - \alpha_0\|$$

Because $q < 1$, p^k will decrease with increasing k, and therefore it is possible to conclude

that (α_k) is a Cauchy sequence. Since K is complete there exists an $\alpha_* \in K$ such that $\alpha_k \longrightarrow \alpha_*$.

we have to obtain p constant from kinetic equation. To show that we will use mean value theorem:

According to mean value theorem for all $x, y \in K$ where $x < y$, that there exists a point c in an open interval (x, y) at which

$$||f(y) - f(x)|| = ||f'(c)||.||y - x|| \leq q||y - x||$$

we can say that for some positive $q \leq 1$, which implies that f is a contraction mapping with a bounded factor q.

If we consider kinetic equation

$$||F(\alpha) - F(\beta)|| \leq \frac{dF}{d\alpha}||\alpha - \beta|| \tag{3.44}$$

we can calculate $\frac{dF}{d\alpha}$

$$\begin{aligned}
\frac{dF}{d\alpha} =& \frac{A}{\beta} exp(-\frac{E}{RT}) f(\alpha) \\
=& f(\alpha) = \alpha^{0.6}(1 - \alpha^{1.4}) \\
\frac{df}{d\alpha} =& -\frac{((1-\alpha)^{(2/5)}(10\alpha - 3))}{5\alpha^{(2/5)}}
\end{aligned}$$

and $0 < \alpha < 1$ and this is our constant $0 < q < 1$.

3.2. Curve Fitting

Curve fitting is the process of define the model that provides the best fit to the specific curves in given for the data. Curved is the relationships between variables which

is given dataset.

3.2.1. The Method of Least Squares

Curve fitting is a very common problem in science and engineering. Suppose that from some experiment N observations values of a dependent variable y measured at specified values of an independent variable x, have been collected. In other words, we have a set of N

$$(x_1, y_1), (x_2, y_2), (x_3, y_3), \ldots, (x_N, y_N) \tag{3.45}$$

for linear function of the form

$$y = f(x) = Ax + B \tag{3.46}$$

we may define the experimental error in the measurements associated to saying

$$e_k = f(x_k) - y_k \qquad for \qquad 1 \leq k \leq N \tag{3.47}$$

We can define several norms that can be used with the errors to measure how far the curve from our data

$$\begin{aligned} Maximum \quad error: \qquad & E_\infty(f) = \max_{\mathbf{1 \leq k \leq N}} \{f(x_k) - y_k\} \\ Average \quad error: \qquad & E_1(f) = \frac{1}{N} \sum_{k=1}^{N} |f(x_k) - y_k| \\ Root - mean - square \quad error: \qquad & E_2(f) = \left(\frac{1}{N} \sum_{k=1}^{N} |f(x_k) - y_k|^2 \right)^{1/2} \end{aligned}$$

Least squares fitting is due to the choice of f parameters to minimize the root mean square error.

For our data set in Eqn.(3.45) and our linear function Eqn.(3.46) the root-mean-square error will be minumum if and only if $N(E_2(f))^2 = \left(\frac{1}{N} \sum_{k=1}^{N} (Ax_k + B - y_k)^2 \right)^2$ is a minumum [20].

Theorem 3.4 (Least-Squares Line) *Suppose that* $\{(x_k, y_k)\}_{k=1}^N$ *are N points, where the abscissas* $\{x_k\}_{k=1}^N$ *are distinct. The coefficients of the least-squares line*

$$y = Ax + B \tag{3.48}$$

is the solution to the following linear system, known as the normal equations:

$$\begin{aligned} \left(\sum_{k=1}^{N} x_k^2\right) A + \left(\sum_{k=1}^{n} x_k\right) B &= \sum_{k=1}^{N} x_k y_k \\ \left(\sum_{k=1}^{N} x_k\right) A + NB &= \sum_{k=1}^{N} y_k \end{aligned} \tag{3.49}$$

Proof We have to minimize the error. Let us define the function

$$E(A, B) = \sum_{k=1}^{N} (Ax_k + B - y_k)^2 \tag{3.50}$$

The minimum value of Eqn.(3.48) is determined by taking partial derivates with respect to A and B equal to zero. We have system of equations

$$0 = \frac{\partial E(A, B)}{\partial A} = 2 \sum_{k=1}^{N} (Ax_k^2 + Bx_k - x_k y_k) \tag{3.51}$$

$$0 = \frac{\partial E(A, B)}{\partial B} = 2 \sum_{k=1}^{N} (Ax_k + B - y_k) \tag{3.52}$$

After doing some arrangements we get the system Eqns.(3.49). □

3.2.2. Data Linearization Technique

When two variables are plotted and the resulting graph is non-linear (power, exponential, or sinusoidal), it is difficult to determine the functional relationship between the two variables from the shape of the curve. However, there is data linearization techniques

that can be used to turn a non-linear equation into a linear one.

Suppose that we are given the points $(x_1, y_1), (x_2, y_2), \cdots, (x_N, y_N)$ and want to fit an exponential curve of the form

$$y = Ce^{Ax} \tag{3.53}$$

First, we will take the logarithm of the both sides and we get

$$\ln(y) = Ax + \ln(C) \tag{3.54}$$

Then, we will do change of variables:

$$\begin{aligned} Y &= \ln y \\ X &= x \\ B &= \ln C \end{aligned}$$

Hence, the new equation is

$$Y = AX + B \tag{3.55}$$

This process is called data linearization [7]. Our normal equations in Eqn.(3.49) becomes

$$\begin{aligned} \left(\sum_{k=1}^{N} X_k^2\right) A + \left(\sum_{k=1}^{N} Y_k\right) B &= \sum_{k=1}^{N} X_k Y_k \\ \left(\sum_{k=1}^{N} X_k\right) A + NB &= \sum_{k=1}^{N} Y_k \end{aligned} \tag{3.56}$$

After A and B have been found, we can compute C as folows:

$$C = e^B$$

We can easily see that in the table (3.1).

Table 3.1. Table of linearization

$y = f(x)$	Linearized form, $Y = Ax + B$	Change of variable(s)
$y = Ce^{Ax}$	$\ln(y) = Ax + \ln(C)$	$X = x, Y = \ln(y), C = e^B$

3.3. A New Numerical Approach: Nonlinear Fitting

Suppose that the experimental data $T = [T_1, T_2 \ldots, T_n]$ and $\alpha = [y_1, y_2, \ldots, y_N]$ temperature and conversion values are given. N is the number of the data. Consider the activation function as follows:

$$\alpha(T) = A(\tanh(B(T_n - C) - 3) + 1) \tag{3.57}$$

where A, B and C are unknowns. We want to fit a function which has a form in Eqn.(3.57). For this purpose, the nonlinear least square method is used. The nonlinear least-square procedure that we find a minimum of

$$E(A, B, C) = \sum_{n=1}^{N} (y_n - A(\tanh(B(T_n - C) - 3) + 1))^2 \tag{3.58}$$

The partial derivative $E(A, B, C)$ with respect to A, B, C are must be zero in order to guarantee minimum of the function given in Eqn.(3.58).

$$\frac{\partial E}{\partial A} = 0, \qquad \frac{\partial E}{\partial B} = 0, \qquad \frac{\partial E}{\partial C} = 0. \tag{3.59}$$

When the all partial derivatives in Eqn.(3.59) are set equal to zero, the resultantly normal equations are obtained:

$$\sum_{n=1}^{N}(-2\tanh(B(T_n - C) - 3)y_n + 2A\tanh(B(T_n - C) - 3) + 2A\tanh(B(T_n - C) - 3)^2) = 0, \tag{3.60}$$

$$\sum_{n=1}^{N}(2AB(\operatorname{sech}(B(T_n - C) - 3)^2 y_n - 2AB\tanh(B(T_n - C) - 3)\operatorname{sech}(B(T_n - C) - 3)^2 - 2AB\operatorname{sech}(B(T_n - C) - 3)^2) = 0, \tag{3.61}$$

$$\sum_{n=1}^{N}(-2AB\operatorname{sech}(B(T_n - C) - 3)^2 y_n + 2AB\operatorname{sech}(B(T_n - C) - 3)^2\tanh(B(T_n - C) - 3) + 2AB\operatorname{sech}(B(T_n - C) - 3)^2) = 0. \tag{3.62}$$

The equations in Eqns.(3.60), (3.61) and (3.62) are the nonlinear system of equations with respect to unknowns A, B, C. The resultantly system can be solved by newton's method method which is given in Eqn.(3.63).

$$z^{k+1} = z^k - J^{-1}(z^k)\begin{pmatrix} F(z^k) \\ G(z^k) \\ S(z^k) \end{pmatrix} \tag{3.63}$$

where $z^k = \begin{pmatrix} A^k \\ B^k \\ C^k \end{pmatrix}$ and J^{-1} is the inverse of the of the Jacobian matrix,

$$J(z) = \begin{pmatrix} \frac{\partial E}{\partial A} & \frac{\partial E}{\partial B} & \frac{\partial E}{\partial C} \\ \vdots & \ddots & \vdots \end{pmatrix}.$$

To start the Newton's iterative method, an initial condition is needed [26]. For convergent A, B and C values we choose appropriate initial condition, $z^0 = \begin{pmatrix} 0 \\ 0 \\ 0 \end{pmatrix}$ and our stopping criteria for $k = 100$.

we will seek values of pre-experimental factor A and activation energy E which are given in Eqn.(2.5). In Eqn.(2.5), there are 4 unknowns and they are A, E, α and $f(\alpha)$.

By using the curve fitting procedure, function given in Eqn.(9) fit the $\alpha(T)$. In the literature there are different choice of $f(\alpha)$. For the model most suitable choice is

$$f(\alpha) = \alpha^m(1-\alpha)^n$$

where m, n are pozitif real numbers. As a result, there are only two unknowns A and E in Eqn.(2.5). To find these unknowns, data linearization technique is used.

The first step is to take the logarithm of both sides of the Eqn.(2.5)

$$\ln\left(\frac{\beta}{f(\alpha)}\right) + \ln\left(\frac{d\alpha}{dT}\right) = \ln(A) - \frac{E}{RT}. \tag{3.64}$$

This results in a linear relation between the new values X and Y:

$$Y = \bar{A} + EX. \tag{3.65}$$

Then introduce the change of variables:

$$Y = \ln\left(\frac{\beta}{f(\alpha)}\right) + \ln\left(\frac{d\alpha}{dT}\right), \qquad \bar{A} = \ln(A), \qquad X = -\frac{1}{RT}. \tag{3.66}$$

CHAPTER 4

SIMULATIONS

4.1. Optimization of Kinetic Parameters

Convection function ($\alpha(T)$) was described as Eqn.(3.57). To start the Newton's iterative method, an initial condition is needed. For convergent A,B and C values appropriate initial condition was chosen.
For calculations, Matlab solver is used (the codes are given in the Appendix section). Finally we obtain the unknown as A,B and C

In this section, it is seeking for values of pre-experimental factor A and activation energy E which are given in Eqn.(2.5). There are four unknows as A, E, α and $f(\alpha)$. The function of $\alpha(T)$ is obtained and $f(\alpha)$ is chosen as $f(\alpha) = \alpha^m(1-\alpha)^n$. To calculate unknowns of the linearization, linear fitting method is used. In Table 4.3, E and A values are given for different samples.
In Table 4.2, E and $\bar{A}$ values are given for different samples. Kinetic analysis was performed by a new mathematical approach based on the nonlinear least square fitting a tanh function and linearization method. This new algorithm is called as a GMN method. Experimentally determined differential scanning calorimetry (DSC) data sets for an epoxy resin functionalized by single wall carbon nanotubes are used for the verification of GMN method. The results obtained from the GMN algorithm are also compared with the methods reported in the literature. Finally, GMN algorithm was in good agreement with experimental data for calculation of the kinetic parameters.

Kissinger method gives average of activation energy for whole process containing all α values.
*The KAS method is an isoconversional method and changes depending on α. The range

Table 4.1. A, B, C obtain from nonlinear fitting and Data Linearization Technique provide getting E, $\ln(A)$ for different β.

Sample No	β	A	B	C	E	$\ln(A)$
1	2.5	0.5	0.0765	358.3126	89.8749	22.2212
1	5	0.5	0.0767	367.8309	85.5814	20.9993
1	10	0.5	0.0608	368.3936	73.3774	17.3604
1	20	0.5	0.0564	377.0870	70.3343	16.4869
2	2.5	0.5	0.0732	356.5693	82.7869	20.0338
2	5	0.5	0.0619	359.3702	71.0760	16.4988
2	10	0.5	0.0558	365.7544	66.7037	15.3149
2	20	0.5	0.0509	374.5726	69.8242	16.2947
3	2.5	0.5	0.0669	352.6327	73.1902	17.1211
3	5	0.5	0.0627	358.7051	68.1392	15.6939
3	10	0.5	0.0545	364.2501	63.2666	14.2895
3	20	0.5	0.0515	375.6366	64.49896	14.6932
4	2.5	0.5	0.0651	353.4174	73.7206	17.7973
4	5	0.5	0.0616	361.2695	76.1108	17.9529
4	10	0.5	0.0596	369.6381	73.5011	17.3437
4	20	0.5	0.0561	380.6521	73.1449	15.7400

Table 4.2. Comparison of the optimum values of GMN method to with Kissinger and KAS* method.

Sample	Kissinger		KAS*		GMN	
No	E	$\ln(A)$	E	$\ln(A)$	E	$\ln(A)$
1	73.6	13.6	75.5 – 61.5	15.2–10.38	73.3774	17.3604
2	66.3	11.3	69.0 – 54.3	13.3 – 8.2	66.7037	15.3149
3	68.1	11.8	61.1 – 51.6	10.6 – 7.8	63.2666	14.2895
4	70.8	12.6	64.9 – 68.6	11.6 – 10.6	73.1449	15.7400

given in the table shows the values corresponding to the α value starting from 0.1 and reaching the value 0.9 with 0.05 increments.

4.2. Simulation of Experimental Data and Numeric Approximations

After optimized the constants A and E, we put that in the Eqn.(2.5). To calculate this differential equation we used 4th order Runge Kutta Method and showed their simulation with experimental data.

4.2.1. For Sample 1

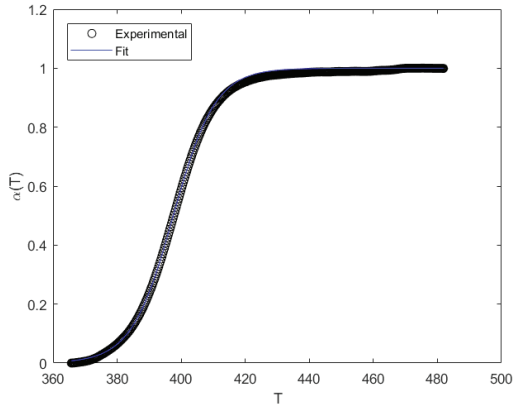

Figure 4.1. Temperature and conversion (α) values are plotted from experimental data and activation function which is used fitting for Sample 1 and $\beta = 2.5$.

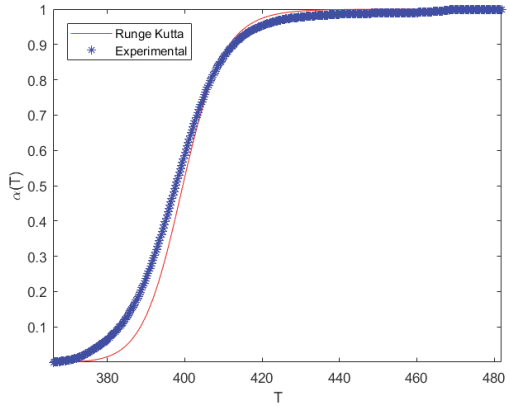

Figure 4.2. Temperature and conversion (α) values are plotted from experimental data and ODE which is used 4th Runge Kutta Method for Sample 1 and $\beta = 2.5$.

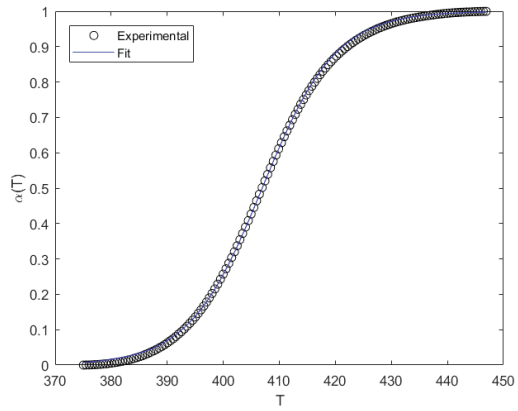

Figure 4.3. Temperature and conversion (α) values are plotted from experimental data and activation function which is used fitting for Sample 1 and $\beta = 5$.

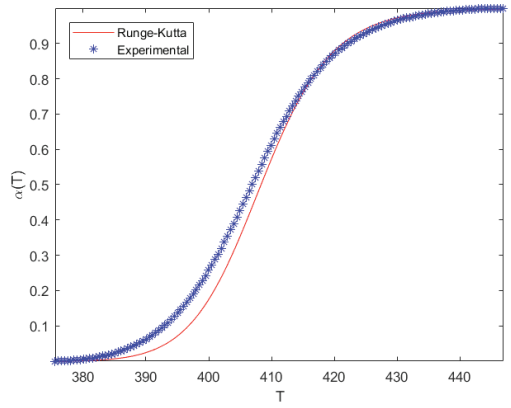

Figure 4.4. Temperature and conversion (α) values are plotted from experimental data and ODE which is used 4th Runge Kutta Method for Sample 1 and $\beta = 5$.

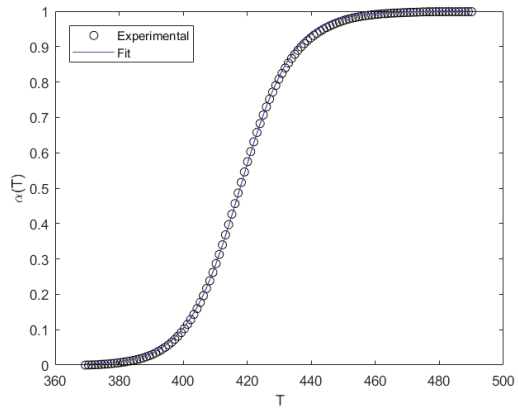

Figure 4.5. Temperature and conversion (α) values are plotted from experimental data and activation function which is used fitting for Sample 1 and $\beta = 10$.

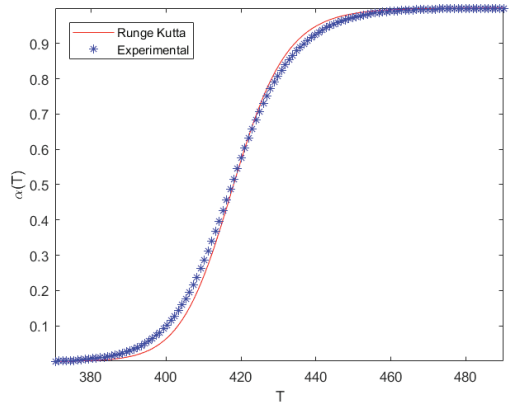

Figure 4.6. Temperature and conversion (α) values are plotted from experimental data and ODE which is used 4th Runge Kutta Method for Sample 1 and $\beta = 10$.

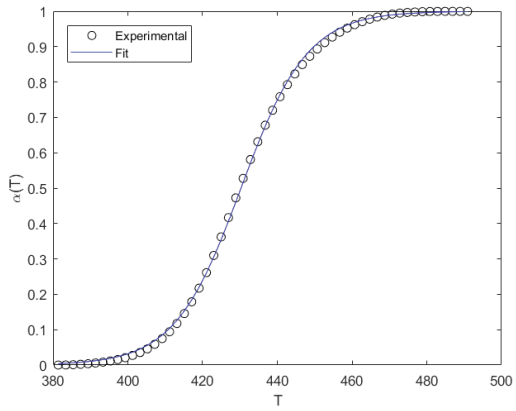

Figure 4.7. Temperature and conversion (α) values are plotted from experimental data and activation function which is used fitting for Sample 1 and $\beta = 20$.

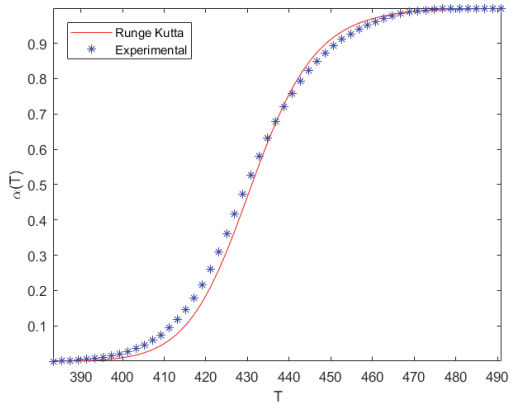

Figure 4.8. Temperature and conversion (α) values are plotted from experimental data and ODE which is used 4th Runge Kutta Method for Sample 1 and $\beta = 20$.

4.2.2. For Sample 2

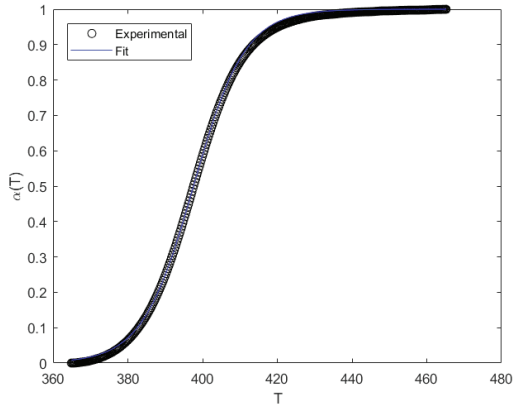

Figure 4.9. Temperature and conversion (α) values are plotted from experimental data and activation function which is used fitting for Sample 2 and $\beta = 2.5$.

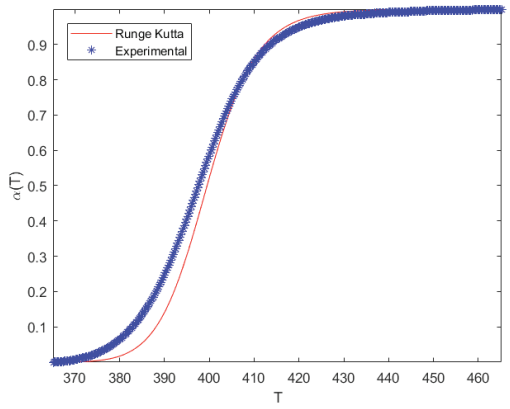

Figure 4.10. Temperature and conversion (α) values are plotted from experimental data and ODE which is used 4th Runge Kutta Method for Sample 2 and $\beta = 2.5$.

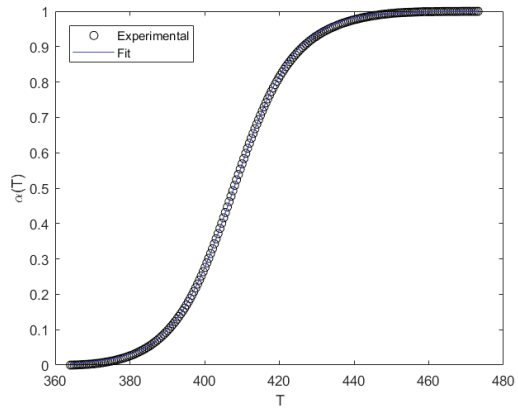

Figure 4.11. Temperature and conversion (α) values are plotted from experimental data and activation function which is used fitting for Sample 2 and $\beta = 5$.

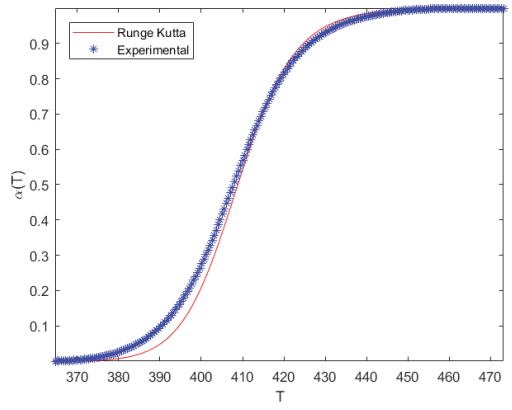

Figure 4.12. Temperature and conversion (α) values are plotted from experimental data and ODE which is used 4th Runge Kutta Method for Sample 2 and $\beta = 5$.

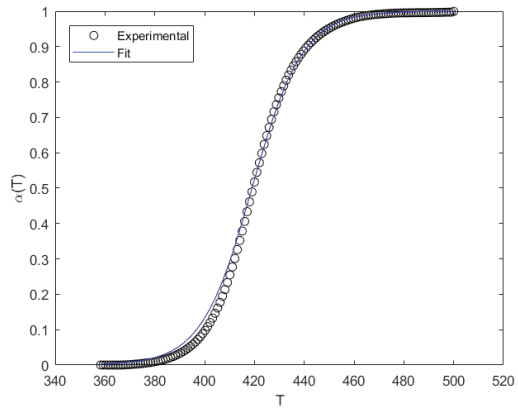

Figure 4.13. Temperature and conversion (α) values are plotted from experimental data and activation function which is used fitting for Sample 2 and $\beta = 10$.

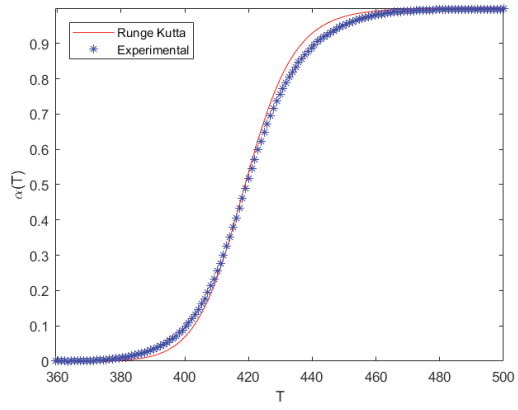

Figure 4.14. Temperature and conversion (α) values are plotted from experimental data and ODE which is used 4th Runge Kutta Method for Sample 2 and $\beta = 10$.

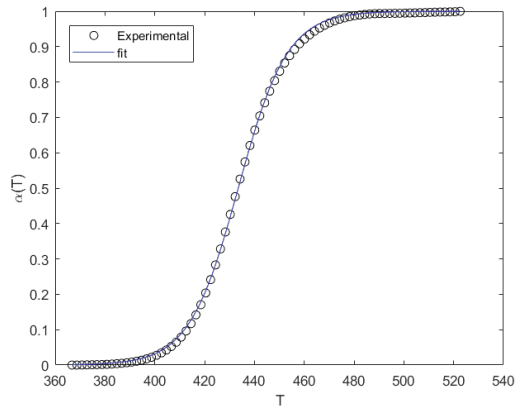

Figure 4.15. Temperature and conversion (α) values are plotted from experimental data and activation function which is used fitting for Sample 2 and $\beta = 20$.

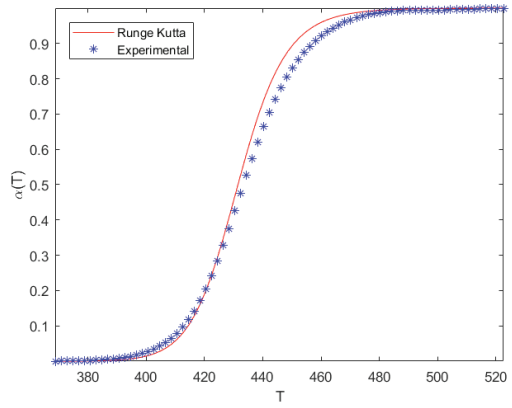

Figure 4.16. Temperature and conversion (α) values are plotted from experimental data and ODE which is used 4th Runge Kutta Method for Sample 2 and $\beta = 20$.

4.2.3. For Sample 3

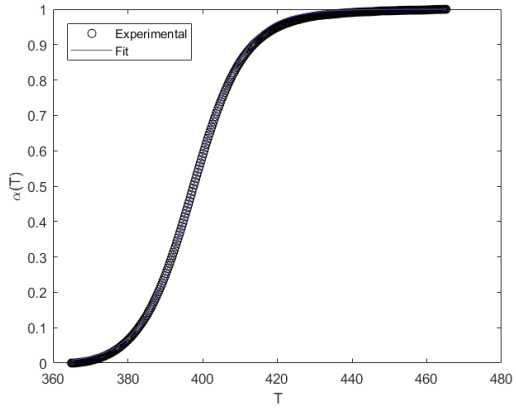

Figure 4.17. Temperature and conversion (α) values are plotted from experimental data and activation function which is used fitting for Sample 3 and $\beta = 2.5$.

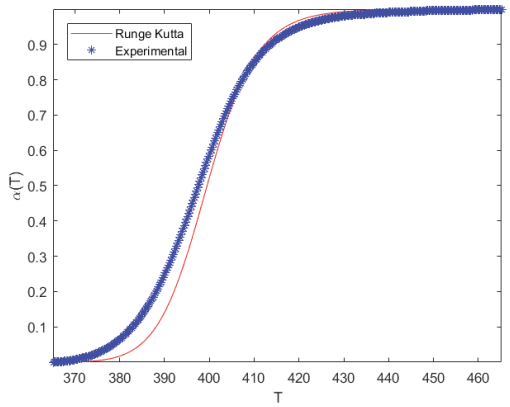

Figure 4.18. Temperature and conversion (α) values are plotted from experimental data and ODE which is used 4th Runge Kutta Method for Sample 3 and $\beta = 2.5$.

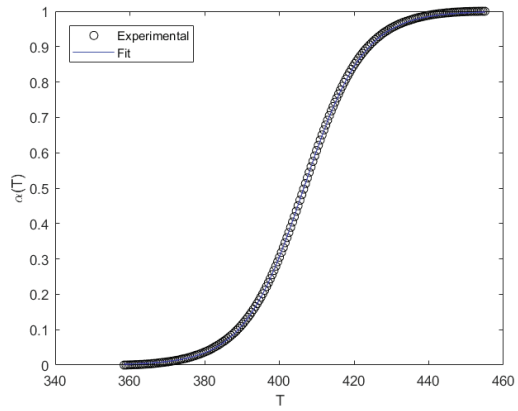

Figure 4.19. Temperature and conversion (α) values are plotted from experimental data and activation function which is used fitting for Sample 3 and $\beta = 5$.

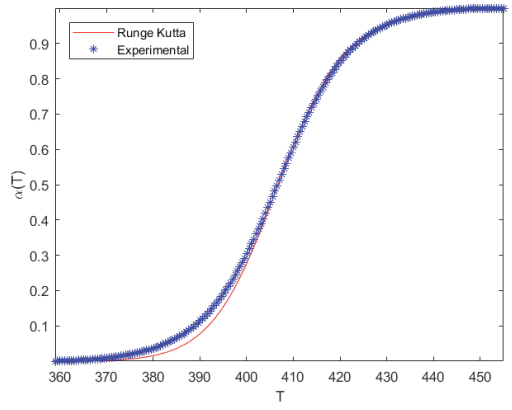

Figure 4.20. Temperature and conversion (α) values are plotted from experimental data and ODE which is used 4th Runge Kutta Method for Sample 3 and $\beta = 5$.

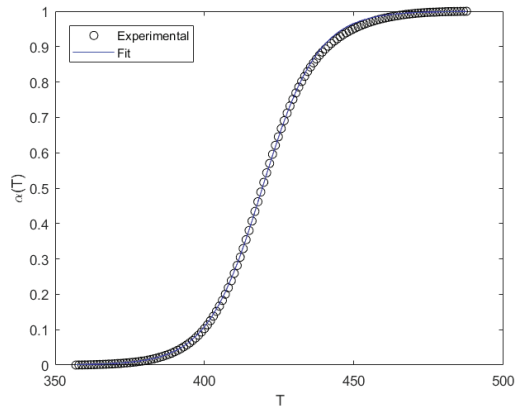

Figure 4.21. Temperature and conversion (α) values are plotted from experimental data and activation function which is used fitting for Sample 3 and $\beta = 10$.

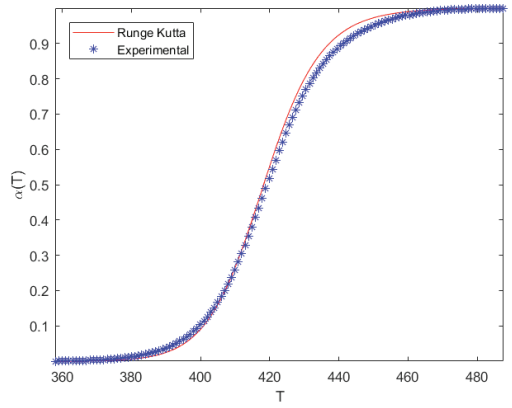

Figure 4.22. Temperature and conversion (α) values are plotted from experimental data and ODE which is used 4th Runge Kutta Method for Sample 3 and $\beta = 10$.

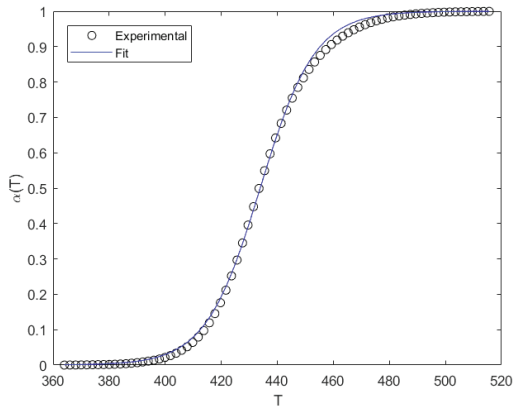

Figure 4.23. Temperature and conversion (α) values are plotted from experimental data and activation function which is used fitting for Sample 3 and $\beta = 20$.

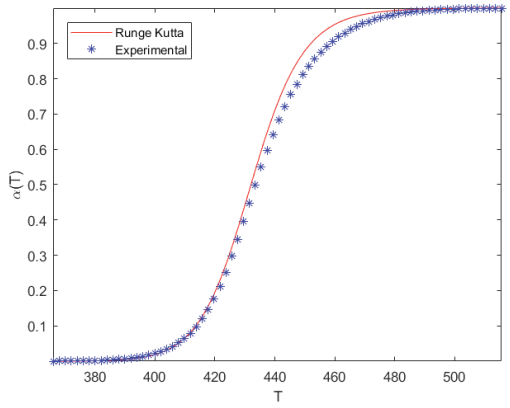

Figure 4.24. Temperature and conversion (α) values are plotted from experimental data and ODE which is used 4th Runge Kutta Method for Sample 3 and $\beta = 20$.

4.2.4. For Sample 4

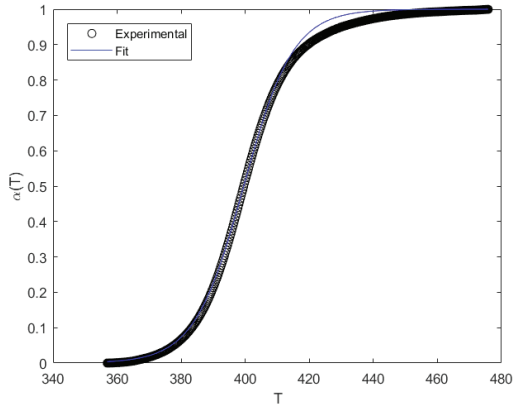

Figure 4.25. Temperature and conversion (α) values are plotted from experimental data and activation function which is used fitting for Sample 4 and $\beta = 2.5$.

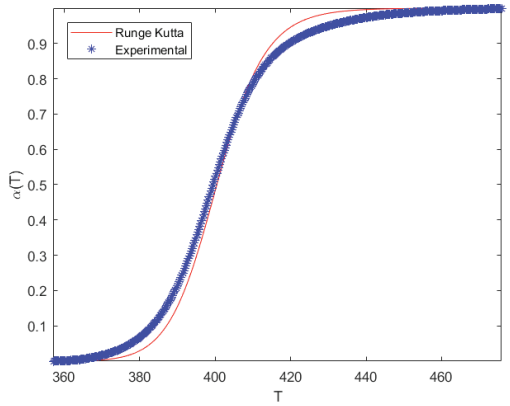

Figure 4.26. Temperature and conversion (α) values are plotted from experimental data and ODE which is used 4th Runge Kutta Method for Sample 4 and $\beta = 2.5$.

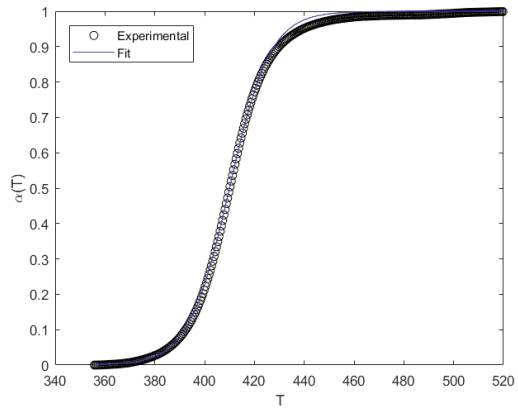

Figure 4.27. Temperature and conversion (α) values are plotted from experimental data and activation function which is used fitting for Sample 4 and $\beta = 5$.

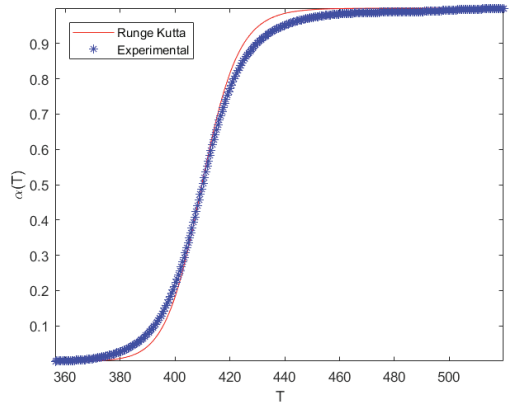

Figure 4.28. Temperature and conversion (α) values are plotted from experimental data and ODE which is used 4th Runge Kutta Method for Sample 4 and $\beta = 5$.

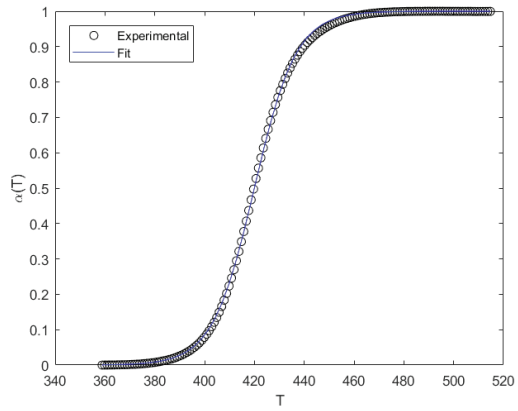

Figure 4.29. Temperature and conversion (α) values are plotted from experimental data and activation function which is used fitting for Sample 4 and $\beta = 10$.

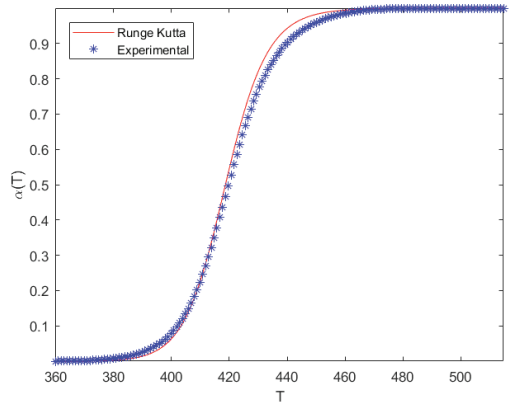

Figure 4.30. Temperature and conversion (α) values are plotted from experimental data and ODE which is used 4th Runge Kutta Method for Sample 4 and $\beta = 10$.

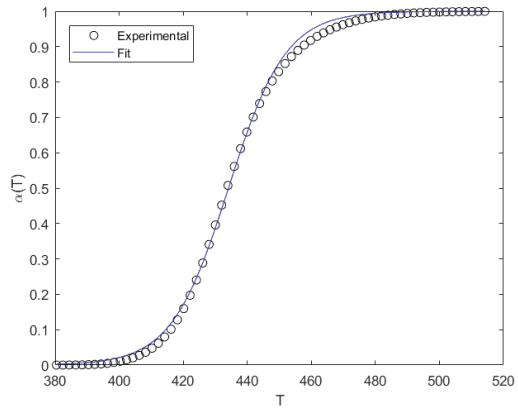

Figure 4.31. Temperature and conversion (α) values are plotted from experimental data and activation function which is used fitting for Sample 4 and $\beta = 20$.

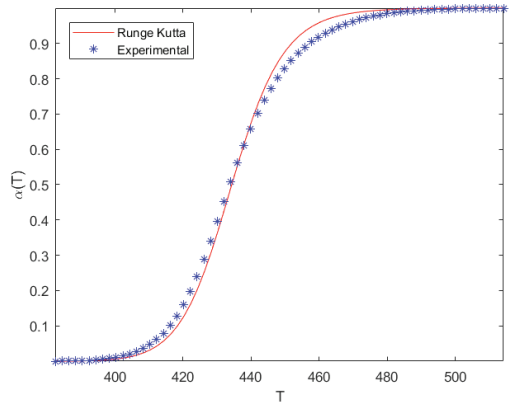

Figure 4.32. Temperature and conversion (α) values are plotted from experimental data and ODE which is used 4th Runge Kutta Method for Sample 4 and $\beta = 20$.

The errors we get using the 4 order Runge Kutta method are listed in the table.

Table 4.3. Error obtain from 4 order Runge Kutta method for different E, $\ln(A)$ and β.

Sample No	β	E	$\ln(A)$	Error
1	2.5	89.8749	22.2212	0.8794
1	5	85.5814	20.9993	0.4824
1	10	73.3774	17.3604	0.2257
1	20	70.3343	16.4869	0.9466
2	2.5	82.7869	20.0338	0.8895
2	5	71.0760	16.4988	0.4245
2	10	66.7037	15.3149	0.2676
2	20	69.8242	16.2947	0.2894
3	2.5	73.1902	17.1211	0.4124
3	5	68.1392	15.6939	0.2575
3	10	63.2666	14.2895	0.2313
3	20	64.49896	14.6932	0.2601
4	2.5	73.7206	17.7973	0.6801
4	5	76.1108	17.9529	0.3527
4	10	73.5011	17.3437	0.1665
4	20	73.1449	15.7400	0.1974

CHAPTER 5

CONCLUSION

In this thesis, we proposed a new algorithm (GMN) for determining pre-exponential and activation energy of curing process. This method is based on the combination of tanh fitting for the measured conversion values via least squares minimization technique and linear fitting for the kinetic parameters. Experimentally determined differential scanning calorimetry (DSC) data sets for an epoxy resin functionalized by single wall carbon nanotubes are used for the verification of the proposed method. After obtaining kinetic parameters we put that constants in the differential equation and solve initial value problem by using 4th order Runge Kutta method. We showed that convergence and stability condition of 4th order Runge Kutta method. Also we demonstrated existence and uniqueness of initial value problem.In computational part, in order to denote the effectiveness of the new proposed method, the results are also compared with the methods reported in the literature. Finally, GMN algorithm was in good agreement with experimental data for calculation of the kinetic parameters.

REFERENCES

[1] C. Arévalo, G. Söderlind, Y. Hadjimichael, and I. Fekete. Local error estimation and step size control in adaptive linear multistep methods. *Numerical Algorithms*, 86:537–563, 2021.

[2] K. Atkinson, W. Han, and D. Stewart. Numerical solution of ordinary differential equations, a john wiley and sons. *Inc., Publication*, 2008.

[3] M. E. Brown, D. Dollimore, and A. K. Galwey. *Reactions in the solid state*. Elsevier, 1980.

[4] F. Buehler and J. Seferis. Effect of reinforcement and solvent content on moisture absorption in epoxy composite materials. *Composites Part A: Applied Science and Manufacturing*, 31(7):741–748, 2000.

[5] X. Chen and B. Ellis. Coatings and other applications of epoxy resins. In *Chemistry and technology of epoxy resins*, pages 303–325. Springer, 1993.

[6] M. L. Costa, E. C. Botelho, J. M. F. d. Paiva, and M. C. Rezende. Characterization of cure of carbon/epoxy prepreg used in aerospace field. *Materials Research*, 8:317–322, 2005.

[7] M. Eraky. curve fitting and interpolation techniques. 02 2018.

[8] B. Francis, S. Thomas, J. Jose, R. Ramaswamy, and V. L. Rao. Hydroxyl terminated poly (ether ether ketone) with pendent methyl group toughened epoxy resin: miscibility, morphology and mechanical properties. *Polymer*, 46(26):12372–12385, 2005.

[9] D. Griffiths and D. Higham. *Numerical methods for ordinary differential equations. Initial value problems*. 01 2010.

[10] R. Hardis, J. L. Jessop, F. E. Peters, and M. R. Kessler. Cure kinetics characterization and monitoring of an epoxy resin using dsc, raman spectroscopy, and dea. *Composites Part A: Applied Science and Manufacturing*, 49:100–108, 2013.

[11] R. Hardis, J. L. Jessop, F. E. Peters, and M. R. Kessler. Cure kinetics characterization and monitoring of an epoxy resin using dsc, raman spectroscopy, and dea. *Composites Part A: Applied Science and Manufacturing*, 49:100–108, 2013.

[12] S. Hirose, T. Hatakeyama, and H. Hatakeyama. Curing and glass transition of epoxy resins from ester-carboxylic acid derivatives of mono-and disaccharides, and alcoholysis lignin. In *Macromolecular Symposia*, volume 224, pages 343–354. Wiley Online Library, 2005.

[13] J. Hodgkin, G. P. Simon, and R. J. Varley. Thermoplastic toughening of epoxy resins: a critical review. *Polymers for advanced technologies*, 9(1):3–10, 1998.

[14] T. Hsieh, A. Kinloch, K. Masania, J. S. Lee, A. Taylor, and S. Sprenger. The toughness of epoxy polymers and fibre composites modified with rubber microparticles and silica nanoparticles. *Journal of materials science*, 45(5):1193–1210, 2010.

[15] K. Hussain, F. Ismail, N. Senu, and F. Rabiei. Fourth-order improved runge–kutta method for directly solving special third-order ordinary differential equations. *Iranian journal of science and technology. transaction a, science*, 41, 11 2015.

[16] H. E. Kissinger. Reaction kinetics in differential thermal analysis. *Analytical chemistry*, 29(11):1702–1706, 1957.

[17] J. Kratz. Transport phenomena in vacuum bag only prepreg processing of honeycomb sandwich panels. 2014.

[18] A. A. Kumar and R. Sundaram. Cure cycle optimization for the resin infusion technique using carbon nanotube additives. *Carbon*, 96:1043–1052, 2016.

[19] J. Martin, A. Cadenato, and J. Salla. Comparative studies on the non-isothermal dsc curing kinetics of an unsaturated polyester resin using free radicals and empirical models. *Thermochimica Acta*, 306(1-2):115–126, 1997.

[20] S. J. Miller. The method of least squares. In *The Probability Lifesaver*, pages 625–635. Princeton University Press, 2017.

[21] M. Öz, G. Tanoglu, N. Imamoglu, Y. Uz, and M. Tanoglu. A new mathematical approach for determining kinetic parameters of curing process. In *9th (Online) International Conference on Applied Analysis and Mathematical Modeling (ICAAMM21) June 11-13, 2021, Istanbul-Turkey*, page 28.

[22] T. Ozawa. Kinetic analysis of derivative curves in thermal analysis. *Journal of thermal analysis*, 2(3):301–324, 1970.

[23] S. T. Peters. *Handbook of composites*. Springer Science & Business Media, 2013.

[24] T. Pozegic, I. Hamerton, J. Anguita, W. Tang, P. Ballocchi, P. Jenkins, and S. R. Silva. Low temperature growth of carbon nanotubes on carbon fibre to create a highly networked fuzzy fibre reinforced composite with superior electrical conductivity. *Carbon*, 74, 03 2014.

[25] W. H. Press. The art of scientific computing 2nd edition in numerical recipes in c, 1997.

[26] C. Remani. Numerical methods for solving systems of nonlinear equations. *Lakehead University Thunder Bay, Ontario, Canada*, 2013.

[27] J. Shen, W. Huang, L. Wu, Y. Hu, and M. Ye. The reinforcement role of different amino-functionalized multi-walled carbon nanotubes in epoxy nanocomposites. *Composites Science and Technology*, 67(15-16):3041–3050, 2007.

[28] N. A. Siddiqui, S. U. Khan, P. C. Ma, C. Y. Li, and J.-K. Kim. Manufacturing and characterization of carbon fibre/epoxy composite prepregs containing carbon nan-

otubes. *Composites Part A: Applied Science and Manufacturing*, 42(10):1412–1420, 2011.

[29] N. A. Siddiqui, S. U. Khan, P. C. Ma, C. Y. Li, and J.-K. Kim. Manufacturing and characterization of carbon fibre/epoxy composite prepregs containing carbon nanotubes. *Composites Part A: Applied Science and Manufacturing*, 42(10):1412–1420, 2011.

[30] P. Šimon. Isoconversional methods. *Journal of Thermal Analysis and Calorimetry*, 76(1):123–132, 2004.

[31] L. T. Sin, W. Rahman, A. Rahmat, and M. Mokhtar. Determination of thermal stability and activation energy of polyvinyl alcohol–cassava starch blends. *Carbohydrate Polymers*, 83(1):303–305, 2011.

[32] V. Slovák and B. Taraba. Urea and cacl2 as inhibitors of coal low-temperature oxidation. *Journal of thermal analysis and calorimetry*, 110(1):363–367, 2012.

[33] M. Stanko and M. Stommel. Kinetic prediction of fast curing polyurethane resins by model-free isoconversional methods. *Polymers*, 10(7):698, 2018.

[34] M. Stanko and M. Stommel. Kinetic prediction of fast curing polyurethane resins by model-free isoconversional methods. polymers. 10 (7): 698, 2018.

[35] M. Vafayan, M. H. Beheshty, M. H. R. Ghoreishy, and H. Abedini. Advanced integral isoconversional analysis for evaluating and predicting the kinetic parameters of the curing reaction of epoxy prepreg. *Thermochimica Acta*, 557:37–43, 2013.

[36] S. Wang, J. He, C. Wang, and X. Li. The definition and numerical method of final value problem and arbitrary value problem. *arXiv preprint arXiv:1801.01608*, 2018.

[37] X. Wu, L. Zhan, S. Li, and W. Li. Study on the cure kinetics of epoxy resin prepreg in fiber metal laminates. In *MATEC Web of Conferences*, volume 88, page 02004.

APPENDIX

```
      %% A(tanh(B(T-C)-3)+1)%%
clear all;close all;clc
function [F,J] = Derivative (p, x, y)
     if nargout > 1;
     J = [(tanh(p(2)*(x-p(3))-3)+1), p(1)*(x-p(3))*(sech(p(2)*(x-p(3))-3).^2),
    -p(1)*p(2)*(sech(p(2)*(x-p(3))-3).^2)];
     end
end
 % Vectors: Y and T
x=T';
y=Y';;
p0=[0; 0; 0];
% Jacobian setting
opts = optimset ('Jacobian', 'on')
% model function:
[x,norm] = lsqnonlin(@(p) Derivative(p, x, y), p0)

  %T and Y are vectors for Sample 1 beta=2.5
TT=T+273; %Kelvin
c1=p(0);
c2=p(1);
n=1.4;
m=0.6;
B=2.5; %C/min
BB=B/60; %K/sec
R=8.314;
y=@(x) 0.5*(tanh(c1*(x-c2)-3)+1);
```

```
ee=max(abs(y(TT)-Y))
xx = linspace(TT(1),TT(end));
figure(1)
plot(TT,Y,'ko',xx,y(xx),'b-')
legend('Experimental','Fit','Location','northwest')
xlabel('T')
ylabel('\alpha(T)')

dy=@(x) 0.5*c1*(sech(c1*(x-c2)-3).^2);
f=@(x) ((0.5*(tanh(c1*(x-c2)-3)+1)).^(m)).*(1-0.5*(tanh(c1*(x-c2)-3)+1)).^(n);
 G=dy(TT)./f(TT);
X=-1./(R*TT);
YY=log(BB*G);
p=polyfit(X,YY,1);
lnA=p(2);
E=p(1)

A1=exp(lnA); % linear fit
fun=@(x,y) (A1/BB)*exp(-E./(R*x)).*(y.^m).*((1-y).^(n));
a=TT(2);
b=TT(end);
x0=TT(2);
N=length(X(2:end))-1;
h=(b-a)/N;
x=a:h:b;
rk4(1)=Y(2);
 for j=1:N
   kk1=h*fun(x(j),rk4(j));
   kk2=h*fun(x(j)+h/2,rk4(j)+(kk1)/2);
   kk3=h*fun(x(j)+h/2,rk4(j)+(kk2)/2);
   kk4=h*fun(x(j)+h,rk4(j)+(kk3));
```

```
   rk4(j+1)=rk4(j)+(kk1+2*(kk2+kk3)+kk4)/6;
 end
figure(2)
plot(x,rk4,'r-')
axis tight
hold on
plot(TT(2:end),Y(2:end),'*b') ;
legend('Runge Kutta','Experimental','Location','northwest')
xlabel('T')
ylabel('\alpha(T)')
```